

Rapid Capture and Extraction of Sweat for Regional Rate and Cytokine Composition Analysis Using a Wearable Soft Microfluidic System

Journal of Investigative Dermatology (2020) ■, ■-■; doi:10.1016/j.jid.2020.05.107

TO THE EDITOR

Sweat is a rich, heterogeneous biofluid that consists of electrolytes (e.g., sodium, chloride, potassium ions), micronutrients (magnesium ion, calcium ion, iron, vitamin c), metabolites (e.g., glucose, lactate, ammonia, urea), hormones (e.g., cortisol, cytokines), and environmental toxins (e.g., ethanol) (Baker et al., 2009; Baker and Wolfe, 2020). Biomarkers in sweat provide insight about underlying physiological and metabolic processes and exhibit changes related to performance, wellness, and health (Baker and Wolfe, 2020). For example, sweat chloride testing is a well-established and routine clinical tool for cystic fibrosis screening in newborns (Gibson and Cooke, 1959; Mishra et al., 2005). More recently, several studies have demonstrated the efficacy and potential of sweat as a target for monitoring drug levels (e.g., levodopa) for therapeutic dosing (Tai et al., 2019), sweat glucose screening in diabetes management (Lee et al., 2017), ethanol levels to assess alcohol intoxication (Gamella et al., 2014), cortisol levels to monitor stress (Torrente-Rodriguez et al., 2020), and lactate concentrations to track hypoxia (Pribil et al., 2014).

Quantitative analysis of sweat composition and dynamics currently relies on, first, capturing the sweat using disposable gauzes, absorbent pads, or microtubes followed by sample extraction through centrifuge and gravimetric tools and, finally, off-site analysis of the collected samples by leveraging standard laboratory-based analytical techniques. Of these, the sweat collection and extraction steps are most prone to introducing errors

arising from sample contamination, evaporation, and spillage, which affects measurement accuracy, especially for the analysis of small proteins and cytokines in sweat (Dai et al., 2013; Katchman et al., 2018). Thus, there is a critical need for uncomplicated and accurate wearable devices that can readily capture sweat in a point-of-care setting (Choi et al., 2018; Ray et al., 2019).

Here, we present a soft, skin-interfaced microfluidic patch that facilitates rapid capture and clean extraction of precise volumes of sweat into quantifiable volumes for cytokine analysis. The microfluidic patches were skin mounted on healthy subjects ($n = 10$) to collect excreted sweat during exposure to heat (40–45 °C) in a controlled environment chamber. The study protocol was approved by the Institutional Review Board of Northwestern University (Evanston, IL) (IRB:STU00208494). Written informed consent was obtained for all subjects. Concentrations of cytokines IL-1 α , IL-1RA, and IL-8 were measured across three regions of the arms for each subject diurnally (morning and evening measurements) and on consecutive days (Supplementary Figure S1). These cytokines were chosen because of their direct relevance to inflammatory responses in patients with atopic dermatitis. Sweat samples were analyzed with an immunoassay, thereby introducing a robust wearable platform for tracking sweat rate and inflammation cytokines found in sweat.

Soft, wearable microfluidic devices and extraction platforms serve as a collection, storage, extraction, and measurement system that is well-

suited for intimate skin coupling and rapid analysis of biofluids in remote settings. The soft wearable device mounts directly on the skin to achieve a water-tight seal. Figure 1a and Supplementary Figure S2 show an exploded view of the multilayered device, highlighting the intricate geometry and ultrathin, impermeable microchannel layers. This six-layer polymeric design is ultrathin and impermeable to external gases, thereby limiting evaporation over several days. This unique material design is ideal for remote clinical trial and at-home settings, where bio-samples may require storage for several hours or days in the absence of biofluid handling equipment. The skin adhesion layer lies on the bottom surface of the device and incorporates a small collection area that facilitates the flow of sweat into an inlet port, which in turn connects to the overlying microchannel. The inlet port is limited in size (1–2 mm), which significantly limits contamination issues owing to sweat-to-skin contact prevalent with more conventional sweat collection devices. Sweat entering the inlet area propagates through the microchannel where it is captured (Figure 1b and c). The length and cross-sectional geometry of the microchannel determine the total volume of sweat captured and sweat rate over a given sweat-collection session. Figure 1d shows three microfluidic patches skin mounted on the forearms of a subject. The magnified view in Figure 1d highlights the key physical features of the patch on the epidermis (e.g., microchannel, inlet port, outlet port) and the real-time flow of sweat through the microchannel in a way that is visible to clinical staff. The extraction platform is used to rapidly extract the collected sweat samples into cryovials

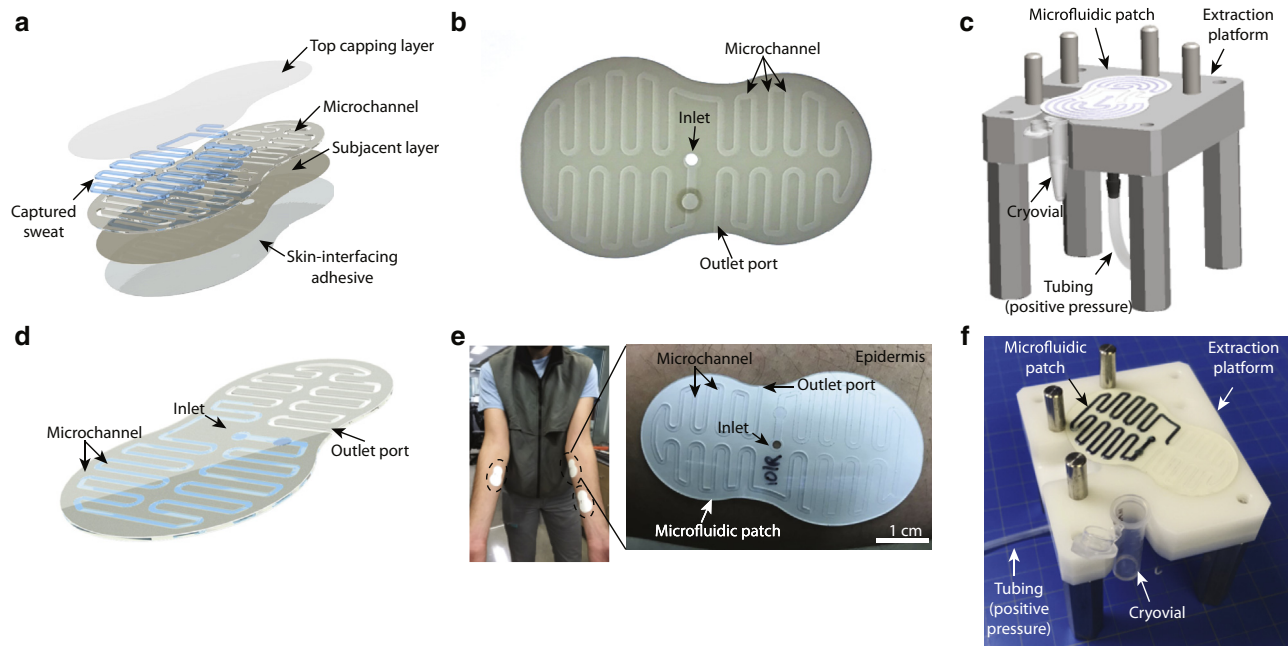


Figure 1. Sweat microfluidics patch. (a) Exploded view of the patch illustrating the multilayered architecture consisting of the top capping layer, microchannels, bottom capping layer, and skin adhesive. (b) Photograph of sweat microfluidics patch showing inlet, outlet port, and microchannel geometry. (c) Schematic drawing of the wearable microfluidic patch and extraction platform showing collected sweat sample being extracted into a cryovial using positive pressure. (d) Three-dimensional rendering of sweat microfluidics patch highlighting the location of the inlet and outlet ports relative to the microchannels. (e) Photograph of subject wearing three microfluidic patches on the inner volar forearms of left and right arms, and at a distal location on the left arm (left panel). Magnified view of microfluidic patch on the inner volar forearm position, attached to the epidermal layer of the skin (right panel). (f) Optical image of the wearable microfluidic patch and extraction platform. The biofluid (blue fluid in the microchannel) is extracted into a cryovial for rapid off-device cytokine analysis.

for analysis, without requiring a centrifuge and other expensive handling equipment (Figure 1e and f and Supplementary Figure S3).

To test the sweat rate dependence of cytokine concentrations, we quantified the volume of sweat collected for each sample. The volumetric range of sweat extracted across multiple subjects was 10–233 μl . Linear regression analysis demonstrates that the volume of collected sweat does not correlate with concentrations of IL-1 α ($y = -7.96x + 2,762$; adjusted $R^2 = 0.08166$) or IL-1RA ($y = -5.97x + 3,449$; adjusted $R^2 = -0.001975$) (Figure 2a). Furthermore, linear regression analysis was conducted for sweat volume and IL-8 ($y = -0.0030x + 1.425$; adjusted $R^2 = 0.0720$); however, the concentrations of IL-8 in sweat in healthy subjects were near the detection limit of the assay, thereby making a correlation difficult to assess in healthy subjects. These volume-versus-concentration results indicate that IL-1 α and IL-1RA concentrations are independent of sweat rate across the forearm regions of the body in healthy subjects.

Because cytokine concentrations in blood plasma have been shown to vary with diurnal cycles (Petrovsky et al., 1998; Vgontzas et al., 2005), we investigated whether a similar phenomenon could be observed with sweat cytokines. Concentrations of IL-1 α and IL-1RA were pooled across three anatomic regions (upper left forearm and bilateral lower forearms) and subgrouped by the time of collection (Figure 2b). For sweat samples that were collected during the morning, the median and SD of IL-1 α , IL-1RA, and IL-8 concentrations were $789 \pm 1,599$, $2,639 \pm 2,797$, and 0.92 ± 0.86 pg/ml, respectively. Concentrations of IL-1 α were comparable with those measured using other sweat collection methods (Dai et al., 2013; Katchman et al., 2018). For sweat samples that were collected during the evening, the median and SD of IL-1 α , IL-1RA, and IL-8 concentrations were $2,639 \pm 1,432$, $2,340 \pm 3,021$, and 1.02 ± 0.25 pg/ml, respectively. Wilcoxon rank-sum tests were conducted to compare the cytokine concentrations between morning and evening sample collections. The differences

between morning and evening measurements were statistically significant for IL-1 α ($P = 0.0052$) and IL-1RA ($P = 0.042$), whereas IL-8 ($P = 0.59$) measurements were not.

Unlike plasma, sweat composition could vary with anatomic location (Baker et al., 2009). We analyzed the location dependence of sweat samples collected in the morning and the evening from the different arm locations (Figure 2c). Kruskal–Wallis ANOVA tests demonstrated no significant differences in sweat cytokines collected from the left lower arm, right arm, or upper left arm for both IL-1 α (morning: $P = 0.58$; evening: $P = 0.97$) and IL-1RA (morning: $P = 0.78$; evening: $P = 0.81$).

The results of Figure 2 provide insight into the origins of IL-1 α and IL-1RA in sweat. The relative independence of cytokine concentrations on sweat rate suggests that the cytokines are present in the sweat produced by the sweat glands rather than dissolved into sweat after being produced by another mechanism (e.g., keratinocytes). This in turn suggests a correlation between cytokine levels in sweat, interstitial

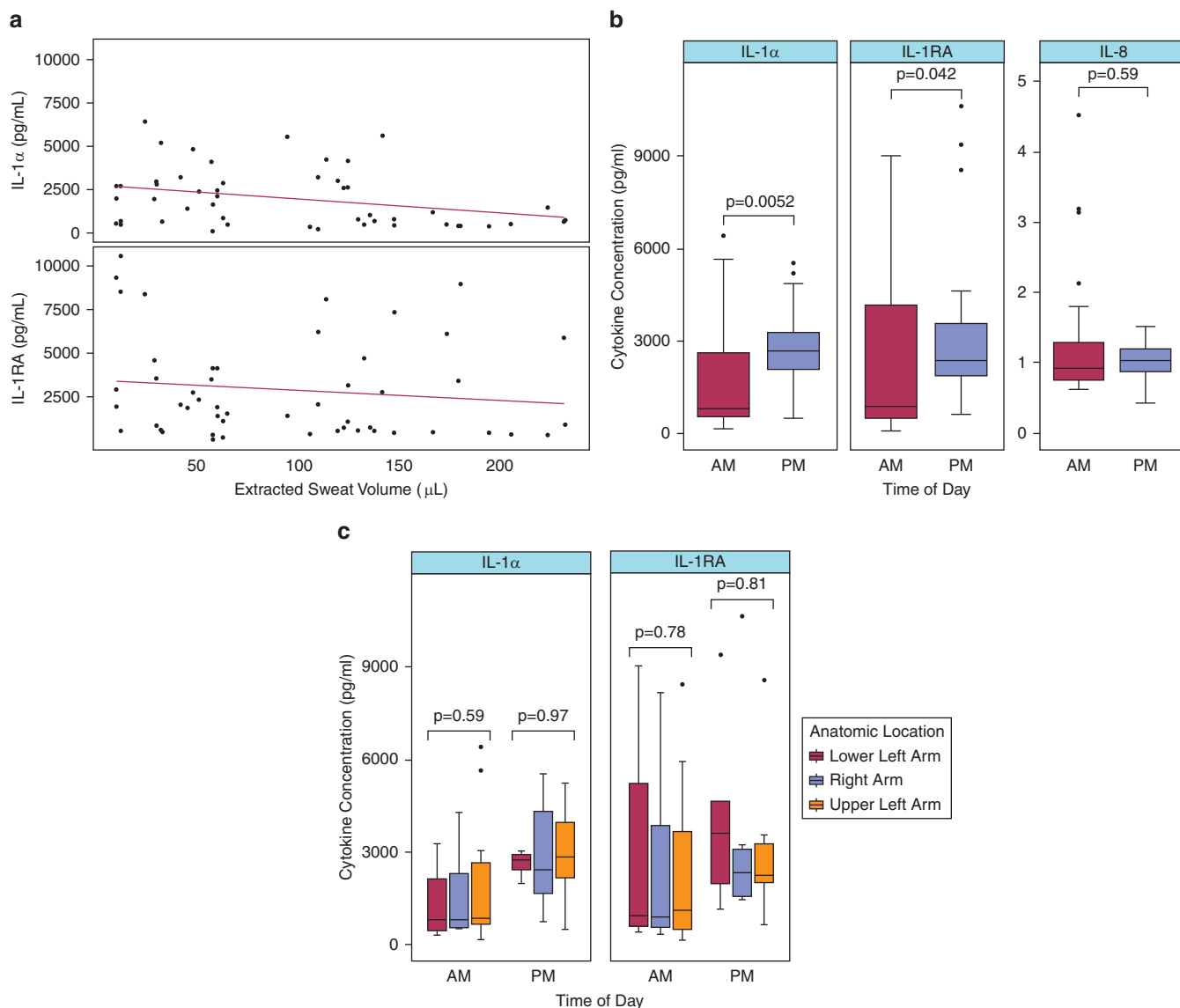


Figure 2. Sweat cytokines rate dependence and concentrations. (a) Linear regression fit for IL-1 α concentration as a function of sweat volume collected ($y = -7.96x + 2,762$; adjusted $R^2 = 0.082$) (Top). Linear regression fit for IL-1RA concentration as a function of sweat volume collected ($y = -5.97x + 3,449$; adjusted $R^2 = -0.0019$) (Bottom). Best fits show that cytokine concentrations are not dependent on volume or rate of sweat extraction. (b) Box and whisker plots showing cytokine concentrations pooled across subjects ($n = 10$ subjects) and body locations. (c) Box and whisker plots for morning and evening collections for IL-1 α (left) and IL-1RA (right) ($n = 10$ subjects). The results show that there are differences as a function of diurnal collection cycles but no differences corresponding to anatomic regions. AM, ante meridiem; PM, post meridiem.

fluid, and plasma, providing a potential noninvasive way to track changes in plasma cytokine levels. The presence of such correlation needs to be established through direct measurements.

The lack of dependence on anatomic collection location (Figure 2c) and consistency across days (Supplementary Figure S1) indicate that cytokine concentrations are consistent over days and locations in healthy subjects but could vary with time of day for a given subject (Figure 2b). The relative increases in IL-1 α and IL-1RA concentrations in the evening

compared with those in the morning indicate diurnal fluctuations in sweat cytokine levels, consistent with previous studies of cytokine plasma and sweat cytokine levels (Katchman et al., 2018; Petrovsky et al., 1998; Vgontzas et al., 2005). Whether such fluctuations serve a skin-specific role or simply reflect variations in plasma concentrations, requires additional testing across larger populations and different disease subgroups, including atopic dermatitis, urticaria, hyperhidrosis, and other autonomic thermal regulation disorders.

Data availability statement

The data that support the plots within this paper and other findings of this study are available from the corresponding author upon reasonable request.

ORCIDi

Jeffrey B. Model: <http://orcid.org/0000-0003-3052-7076>

Michael Z. Zhang: <http://orcid.org/0000-0002-7485-8101>

Adam Leech: <http://orcid.org/0000-0003-3943-1097>

Weihua Li: <http://orcid.org/0000-0001-5660-5082>

Melissa S. Seib: <http://orcid.org/0000-0002-9528-0118>

Shulin Chen: <http://orcid.org/0000-0002-0280-1536>

Jessica Wallace: <http://orcid.org/0000-0002-2654-7149>
 Michael H. Shin: <http://orcid.org/0000-0002-8803-6862>
 Amay J. Bhandodkar: <http://orcid.org/0000-0002-1792-1506>
 Jungil Choi: <http://orcid.org/0000-0002-3659-8978>
 Amy S. Paller: <http://orcid.org/0000-0001-6187-6549>
 John A. Rogers: <http://orcid.org/0000-0002-2980-3961>
 Shaui Xu: <http://orcid.org/0000-0003-3560-6945>

CONFLICT OF INTEREST

AJA, JBM, SPL, AL, WL, NR, MSS, SC, JW, JAR, and RG are cofounders and/or employees of Epicore Biosystems, Cambridge, MA, a company that pursues commercialization of microfluidic devices for wearable applications. The remaining authors state no conflict of interest.

ACKNOWLEDGMENTS

This research was funded by LEO Science & Tech Hub. This work utilized the Northwestern University Micro/Nano Fabrication Facility.

AUTHOR CONTRIBUTIONS

Conceptualization: AJA, JBM, SPL, JAR, ASP, SX, RG; Data Curation: AJA, MZZ, SPL; Formal Analysis: AJA, MZZ, SPL, RG; Investigation: WL, SC, JC, AJA, MSS, SPL, AJB, RG; Methodology: JBM, AL, NR, JW; Writing - Original Draft Preparation: AJA, MZZ, RG; Writing - Review and Editing: AJA, JBM, SPL, NR, MZZ, MSS, AJB, JW, JAR, ASP, SX, RG

Alexander J. Aranyosi^{1,2,3,9}, Jeffrey B. Model^{1,2,3,9}, Michael Z. Zhang^{4,9}, Stephen P. Lee^{1,2,3}, Adam Leech¹, Weihua Li^{1,2,3}, Melissa S. Seib¹, Shulin Chen^{1,2,5}, Nikolas Reny¹, Jessica Wallace¹, Michael H. Shin⁴, Amay J. Bhandodkar^{2,3,5}, Jungil Choi⁶, Amy S. Paller^{3,4}, John A. Rogers^{2,3,5,7,8}, Shuai Xu^{2,3,4,7} and Roozbeh Ghaffari^{1,2,3,7,8,*}

¹Epicore Biosystems, Cambridge, Massachusetts, USA; ²Querrey Simpson Institute for Bioelectronics, Northwestern University, Evanston, Illinois, USA; ³Center for Bio-Integrated Electronics, Northwestern University, Evanston, Illinois, USA; ⁴Department of Dermatology, Feinberg School of Medicine, Northwestern University, Chicago, Illinois, USA; ⁵Department of Materials Science and Engineering, Northwestern University, Evanston, Illinois, USA; ⁶School of Mechanical Engineering, Kookmin University, Seoul, Republic of Korea; ⁷Department of Biomedical Engineering, Northwestern University, Evanston, Illinois, USA; and ⁸Institute for Innovations in Development Science, Northwestern University, Evanston, Illinois, USA
 *These authors contributed equally to this work.
 *Corresponding author e-mail: rooz@northwestern.edu

SUPPLEMENTARY MATERIAL

Supplementary material is linked to the online version of the paper at www.jidonline.org, and at <https://doi.org/10.1016/j.jid.2020.05.107>.

REFERENCES

- Baker LB, Stofan JR, Hamilton AA, Horswill CA. Comparison of regional patch collection vs. whole body washdown for measuring sweat sodium and potassium loss during exercise. *J Appl Physiol* (1985) 2009;107:887–95.
- Baker LB, Wolfe AS. Physiological mechanisms determining eccrine sweat composition. *Eur J Appl Physiol* 2020;120:719–52.
- Choi J, Ghaffari R, Baker LB, Rogers JA. Skin-interfaced systems for sweat collection and analytics. *Sci Adv* 2018;4:eaar3921.
- Dai X, Okazaki H, Hanakawa Y, Murakami M, Tohyama M, Shirakata Y, et al. Eccrine sweat contains IL-1 α , IL-1 β and IL-31 and activates epidermal keratinocytes as a danger signal. *PLoS One* 2013;8:e67666.
- Gamella M, Campuzano S, Manso J, González de Rivera G, López-Colino F, Reviejo AJ,

et al. A novel non-invasive electrochemical biosensing device for in situ determination of the alcohol content in blood by monitoring ethanol in sweat. *Anal Chim Acta* 2014;806:1–7.

Gibson LE, Cooke RE. A test for concentration of electrolytes in sweat in cystic fibrosis of the pancreas utilizing pilocarpine by iontophoresis. *Pediatrics* 1959;23:545–9.

Katchman BA, Zhu M, Blain Christen J, Anderson KS. Eccrine sweat as a biofluid for profiling immune biomarkers. *Proteomics Clin Appl* 2018;12:e1800010.

Lee H, Song C, Hong YS, Kim MS, Cho HR, Kang T, et al. Wearable/disposable sweat-based glucose monitoring device with multistage transdermal drug delivery module. *Sci Adv* 2017;3:e1601314.

Mishra A, Greaves R, Massie J. The relevance of sweat testing for the diagnosis of cystic fibrosis in the genomic era. *Clin Biochem Rev* 2005;26:135–53.

Petrovsky N, McNair P, Harrison LC. Diurnal rhythms of pro-inflammatory cytokines: regulation by plasma cortisol and therapeutic implications. *Cytokine* 1998;10:307–12.

Pribil MM, Laptev GU, Karyakina EE, Karyakin AA. Noninvasive hypoxia monitor based on gene-free engineering of lactate oxidase for analysis of undiluted sweat. *Anal Chem* 2014;86:5215–9.

Ray TR, Choi J, Bhandodkar AJ, Krishnan S, Gutruf P, Tian L, et al. Bio-integrated wearable systems: a comprehensive review. *Chem Rev* 2019;119:5461–533.

Tai LC, Liaw TS, Lin Y, Nyein HYY, Bariya M, Ji W, et al. Wearable sweat band for noninvasive levodopa monitoring. *Nano Lett* 2019;19:6346–51.

Torrente-Rodríguez RM, Tu J, Yang Y, Min J, Wang M, Song Y, et al. Investigation of cortisol dynamics in human sweat using a graphene-based wireless mHealth system. *Matter* 2020;2:921–37.

Vgontzas AN, Bixler EO, Lin HM, Prolo P, Trakada G, Chrousos GP. IL-6 and its circadian secretion in humans. *Neuroimmunomodulation* 2005;12:131–40.

SUPPLEMENTARY MATERIALS AND METHODS

Sweat collection

Sweat was collected from subjects ($n = 10$) over a 30–45 minutes period on each of two consecutive days (Supplementary Figure S1). For six of these subjects, the collection was conducted at around the same time each day (five in the morning, one in the evening). For the others, sweat was collected during a morning session and evening session. A custom-built microfluidic patch (Supplementary Figure S2a) designed to collect up to ~ 200 μl of sweat, with minimal evaporation (Supplementary Figure S2b), was applied to the epidermis at multiple anatomic positions on the arms.

Subjects' left and right inner volar forearms were examined to ensure that they had intact skin. Subjects with excessive hair in patch application areas had this hair trimmed. The left and right volar forearms were cleaned with sterile alcohol wipes and allowed to dry. Three microfluidic patches were applied to the left proximal, left distal, and right proximal volar forearms (Figure 1d).

Subjects entered a sauna to induce sweating. They were allowed to enter and leave ad libitum until 45 minutes had expired or the patches were filled to at least 50 μl , whichever came first. For the first three subjects, sweat was collected until the patches were completely full to ensure that sufficient sweat was available for assay development. Times of patch application and each sauna entry and exit were recorded.

Sweat extraction

Once subjects exited the sauna, patches were removed one at a time

and placed on a sweat extraction fixture (Supplementary Figure S3a–c). The exit port of the patch was gently cleaned with an alcohol wipe and positioned over the inlet of a labeled cryovial. Positive pressure applied to the fixture pushed sweat through the channel, out of the exit port and into the cryovial (Supplementary Figure S3d). After closing the vial, the patch was removed and discarded, and the extraction fixture was cleaned with an alcohol wipe. This process was repeated for all patches and subjects for a given collection group.

To determine collected sweat volume, a scale was zeroed with an empty cryovial and the differential weight of each filled vial was measured. When the fluid volume was very low (~ 15 μl or less), the resulting weight was sometimes zero or negative owing to variation among the vials. Protease and phosphatase inhibitor cocktails were each added at 10% v/v. Vials were then vortexed and stored at -80 $^{\circ}\text{C}$. When all subject samples had been collected and prepared, the samples were shipped overnight on dry ice to a bioassay laboratory (Pacific BioLabs, Hercules, CA) for analysis.

Assay development and cytokine measurements

Sweat was analyzed using U-PLEX assay kits (Meso Scale Diagnostics, Rockville, MD). Because these kits were not designed specifically for sweat, a series of spike-recovery tests were performed to refine and validate the measurement process. For the resulting process, the samples were rapidly thawed and centrifuged. The

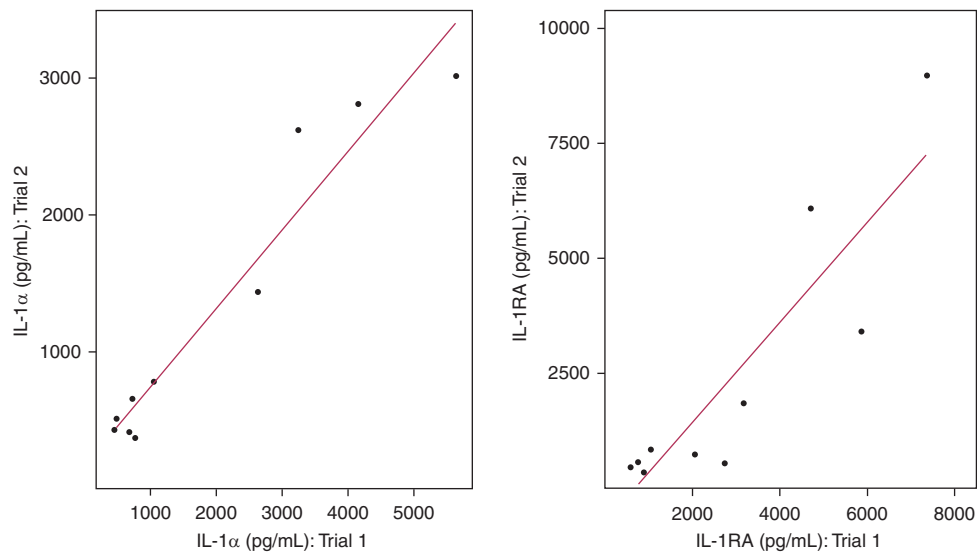
supernatant was extracted and diluted in the ratio of 1:2 in PBS to raise the pH. The samples were then processed following the instructions in the kit. Subject samples were analyzed following this same process.

Diurnal cytokine measurements

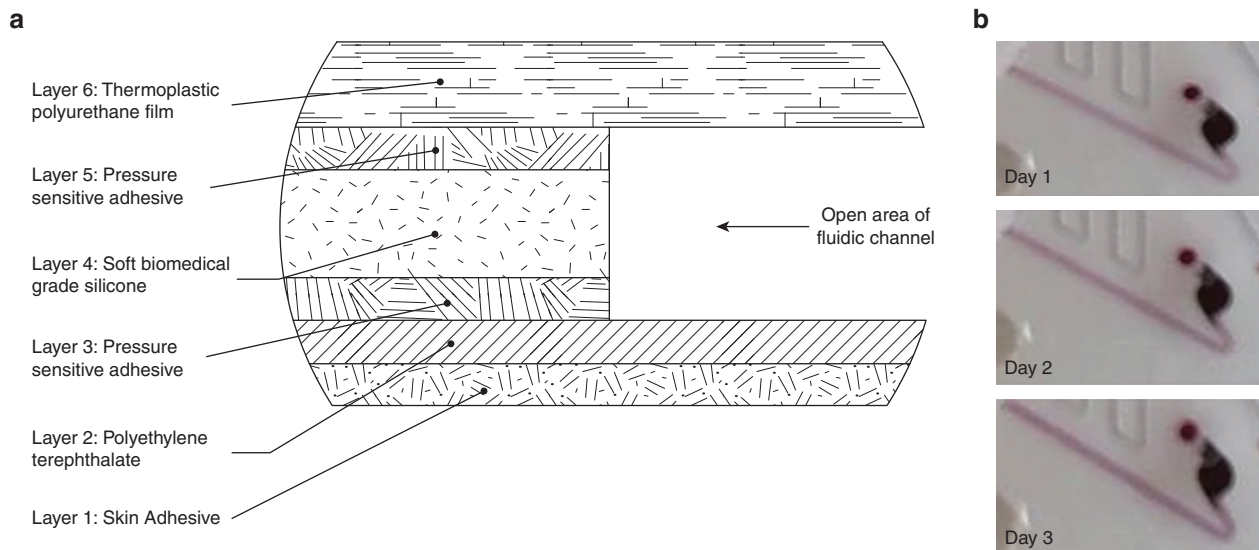
Three subjects had sweat samples collected during both morning and evening, and the cytokine concentrations were directly compared. In all cases, concentrations of IL-1 α and IL-1RA from samples collected in the evening were higher for a given subject. Mean ratios (evening to morning) were 4.2 for IL-1 α (range 1.4–5.8) and 4.6 for IL-1RA (range 2.7–5.5). In one subject from whom three samples were collected, concentrations rose from morning to evening on the first day, then fell again the following morning (IL-1 α : 857–3,982–603 pg/ml; IL-1RA: 733–3,267–456 pg/ml).

Consecutive day cytokine measurements

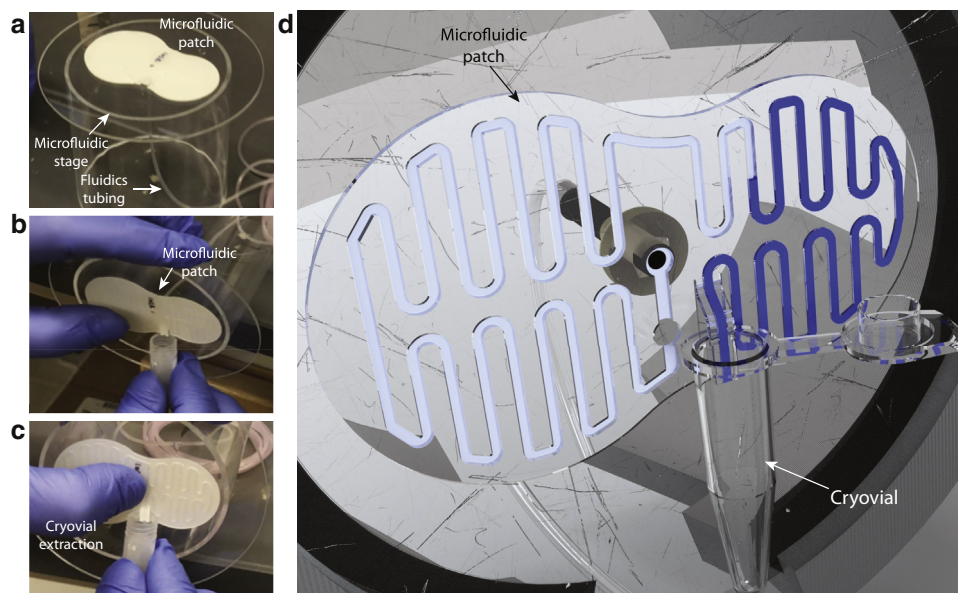
To explore the repeatability of sweat cytokine measurements, samples were collected from each subject on two sequential days. For the purpose of this comparison, only samples collected at the same time of the day (both in the morning or both in the evening) were included. Supplementary Figure S1 shows that IL-1 α and IL-1RA concentrations were highly correlated across days for healthy subjects. However, the slope of the linear regression fit for IL-1 α was less than one (~ 0.57), indicating a shift in concentrations by a factor of ~ 2 across a small sample size.



Supplementary Figure S1. Repeatability of cytokine concentration measurements on two consecutive days. Linear regressions for IL-1 α ($y = 0.57x + 174$, $R^2 = 0.929$; left panel) and IL-1RA ($y = 1.1x - 730$, $R^2 = 0.779$; right panel) show good correlation across trials.



Supplementary Figure S2. Microfluidic patch with soft, flexible, multilayered design. (a) Schematic drawing showing the six-layer polymeric design of the microfluidic patch. The multiple layers protect biofluids from evaporation effects over multiple days of storage. (b) Optical images of artificial sweat samples stored in the microfluidic patch channel for 3 days, with minimal evaporative effects.



Supplementary Figure S3. Microfluidic extraction fixture. (a) Image of sweat microfluidic patch mounted on microfluidic stage after sweat collection on the skin. Tubing is connected to the microfluidic patch inlet port on stage and to a syringe (not shown). (b) Image of a cryovial aligned with the exit port of the microfluidic patch. (c) Positive pressure applied with a syringe at the inlet port pushed sweat through the microfluidic patch and into the cryovial. (d) Schematic illustration showing a wearable microfluidic patch and extraction platform with sweat (denoted in blue) being collected in a cryovial for off-device analysis.